Spatial recurrence analysis: A sensitive and fast detection tool in digital mammography

T. L. Prado, P. P. Galuzio, S. R. Lopes, and R. L. Viana

Citation: Chaos: An Interdisciplinary Journal of Nonlinear Science **24**, 013106 (2014); doi: 10.1063/1.4861895
View online: http://dx.doi.org/10.1063/1.4861895
View Table of Contents: http://scitation.aip.org/content/aip/journal/chaos/24/1?ver=pdfcov
Published by the AIP Publishing

Spatial recurrence analysis: A sensitive and fast detection tool in digital mammography

T. L. Prado, P. P. Galuzio, S. R. Lopes, and R. L. Viana[a)]
Departamento de Física, Universidade Federal do Paraná, 81531-990 Curitiba, Paraná, Brazil

(Received 7 November 2013; accepted 30 December 2013; published online 14 January 2014)

Efficient diagnostics of breast cancer requires fast digital mammographic image processing. Many breast lesions, both benign and malignant, are barely visible to the untrained eye and requires accurate and reliable methods of image processing. We propose a new method of digital mammographic image analysis that meets both needs. It uses the concept of spatial recurrence as the basis of a spatial recurrence quantification analysis, which is the spatial extension of the well-known time recurrence analysis. The recurrence-based quantifiers are able to evidence breast lesions in a way as good as the best standard image processing methods available, but with a better control over the spurious fragments in the image. © *2014 AIP Publishing LLC*.
[http://dx.doi.org/10.1063/1.4861895]

The characterization of spatial profiles has a plethora of applications, ranging from the analysis of turbulent data in astrophysical images to the detection of structures in medical images, like those obtained from MRI and tomography. In the latter case, it is a key problem to identify small structures in mammographies, which are barely visible to the untrained human eye. Such structures may or may not be associated with initial stages of breast cancer, the most common type of cancer in women throughout the world and which is successfully treated if detected in its first stages. Hence the identification of small structures like micro-calcification and masses in mammographic images is an important factor to improve breast cancer diagnostics and treatment. We propose a method of detection of spatial structures in images based on the concept of spatial recurrences, which has been inspired in similar methods used in the analysis of time signals from complex dynamical systems. We show that this method is able to characterize small structures in mammographies using a relatively small computer time, what constitutes itself in a valuable tool for the use of physicians diagnosing possible structures related to breast cancer. We choose this particular application due to the capability of recurrence-based diagnostics to detect small and barely distinguishable structures. However the range of the applications of recurrence-based diagnostics like the ones we presented here is wide and encompasses many fields of applied sciences where image analysis is important.

I. INTRODUCTION

Digital mammography is a radiological investigation of the breast, producing a high-resolution digital image which can be analyzed using computer-aided diagnosis schemes.[1] Fast and reliable computer-aided methods of detection and characterization of lesions can improve the diagnosis of breast cancer, for it provides the clinician with additional and quantitative information, so reducing the presence of false-positive mammographies and the corresponding biopsies of benign lesions.[2] In particular, it is quite difficult for the clinician to distinguish clustered micro-calcifications (in the 0.1–0.5 mm range) and masses in mammographies, in such an extent that between 15% and 30% of such lesions may be missed.[3]

The computer-aided mammographic diagnosis of clustered micro-calcifications is based on difference-image techniques with a set of suitable filters for signal extraction like gray-level thresholding and morphological erosion. Different techniques of feature extraction, like texture, size contrast, shape, edge gradient, and spatial detection, are necessary to distinguish micro-calcification from normal patterns and image noise.[4] For detection and characterization of masses there have been used nonlinear bilateral subtraction techniques.[5] The likelihood of malignancy in both cases is evaluated through using artificial neural networks.[6]

Given the current need of increasingly accurate, fast, and reliable computer-aided techniques of digital mammography analysis, new approaches to this problem are welcome. In this note we propose such a technique, using the recently developed concept of spatial recurrence plots (SRP).[7,8] The latter are based on the idea of recurrence plots (RP), which have been originally introduced as a numerical tool to investigate dynamical patterns in time series.[9] The basic idea of a RP is to start from a phase space embedding (using delay coordinates, for example) and compare the embedding vectors with each other, drawing pixels in a square matrix when the Euclidean distance between vectors is below some threshold.

SRPs are extension of RPs to spatially extended systems by considering space-separated vectors obtained from a given spatial pattern at a fixed time. The spatial proximity of such vectors provides a measure of spatial recurrence for a certain pattern. We then adapted the recurrence quantification analysis techniques, like the determinism and laminarity, to the

[a)]Author to whom correspondence should be addressed. Electronic mail: viana@fisica.ufpr.br

detection of spatial patterns like plateaus, ramps, and disordered structures.[7] SRPs seem to be particularly useful in complex patterns, which are neither entirely smooth nor totally irregular.[10] We applied computer-based spatial recurrence techniques to digital mammography high-resolution images, showing subtle details which escape to visual inspections. We thus claim that SRPs can be used along with the other existing computer-aided techniques so as to provide clinicians additional information for better diagnoses of malignant tumors and other breast lesions.

High-resolution digitalized mammography images were obtained from Ref. 11, which is a widely used access-free site which purports to facilitate sound research in the development of computer algorithms to aid in mammography screening. Conventional methods for image treatment and filtering as degree method, the directional degree method like Sobel, Robert, or Prewitt filters, and Canny edges method for borders[12,13] usually have the advantage to mark only the transitions between quantizations of pixels, but that is also at same time a bad issue because there is a lot of transitions in an image that have no physical meaning. With the Canny edge algorithm there is a control of fragments but is not so easy to define a good threshold that do not eliminate also the important elements in the image. It is in this context that we can use the SRPs, with the help of the optimum algorithm for the threshold it is possible to automatically get rid off the fragments, and maintain the meaningful elements in the image.

The method of image analysis through spatial recurrence quantifiers we introduce in this paper is rather general and can be used in a variety of applications, especially those in which the identification of small and/or barely detectable structures is important. Image analysis is extensively used in biological and medical physics, like in MRI, tomography, and mammography.[14] We have used in this paper representative examples from mammographic images, for which we claim that spatial recurrence-based diagnostics are at least as good as conventional methods for image treatment of mammographic images, with some possible advantages in terms of the computer time required to perform the image reconstruction. Given these advantages, recurrence-based image analysis can be used in other biomedical image processing applications.

This paper is organized as follows: in Sec. II we introduce the recurrence rate matrix description by considering lines and columns of the original image. This procedure is generalized to square blocks in Sec. III. Section IV presents results of image interpretation of mammographic images using block-recurrence analysis. The Sec. VI is devoted to our conclusions.

II. LINE-RECURRENCE ANALYSIS

Scanned mammographic images[1,15,16] are usually stored in data formats like ljpeg or tiff, without changes due to algorithms of optimization and/or compression. We have transformed such images into $K \times M$ matrices with integer entries $1 < a_{ij} < A$, with $i = 1, 2, \ldots K$, $j = 1, 2, \ldots M$, and A is the maximum number of gray levels compatible with the image format (for sake of comparison, in a `jpeg` format the number of red-green-blue (RGB) color levels are 256 for each color channel, but in a lossless image file A can be as large as, e.g., 65 000). From this integer grey level matrix we extract strings of N elements, which are normalized real numbers

$$x_{ij} = \frac{a_{ij} - 1}{A}, \tag{1}$$

such that $0 < x_{ij} < 1$, where $i = 1, 2, \ldots K$ for fixed j or $j = 1, 2, \ldots M$ for fixed i, by picking up some of their lines or columns.[1] These strings form a spatial series $\{x(1), x(2), \ldots x(N)\}$. The value of N varies from 15 to 25 according to the resolution of the original picture.

These spatial series can be analyzed by standard methods in order to unveil patterns of interest in the diagnostics of mammographic images. In this work we propose the use of a technique, called spatial recurrence analysis, that has been borrowed from time series analysis: in the latter we pick up two temporally separated events and consider whether or not they are far apart more than a specified tolerance. If so, they are called recurrent, in the classical mathematical sense of Poincaré. Here we consider the time as being fixed, and we interpret the spatial separation of points in terms of spatial recurrences.

Spatial recurrences can be visualized by using two space-separated points $x(i)$ and $x(j)$ belonging to the N-element strings above. A spatial recurrence matrix has elements R_{ij} equal to 1 if $|x(i) - x(j)| < \epsilon$, and 0 otherwise. In other words, two points $x(i)$ and $x(j)$ are considered as spatially recurrent if they are far apart by a distance smaller than ϵ. Two points for which $x(i) = x(j)$ would be trivially recurrent and add not much useful information, so that it is important to exclude such situations.

This is performed by thresholding the recurrence interval by imposing a very small, yet nonzero, lower bound on the cutoff radius ϵ_{min}. This lower bound is responsible for noise reduction in the final image, since small-amplitude fluctuations fall below this threshold and are thus ignored in the obtention of the spatial recurrence matrix. Likewise we choose an upper bound ϵ_{max} for the cutoff radius. It turns out that ϵ_{min} and ϵ_{max} play roles similar to low-pass and high-pass filters, respectively.

The elements of the spatial recurrence matrix are thus defined as

$$R_{ij} = \Theta\left(|x_i - x_j| - \epsilon_{min}\right)\Theta\left(\epsilon_{max} - |x_i - x_j|\right), \tag{2}$$

where Θ is the Heaviside unit-step function.

SRPs are graphical representations of the recurrence matrix R_{ij}, in the sense that the binary values in R_{ij} are represented by a matrix plot with black (white) pixels when R_{ij} is equal to 1 (0). The use of optimized values for the cutoff radii ϵ_{min} and ϵ_{max} is particularly important if we are to standardize the procedures involved in the recurrence quantification analysis. If we choose values of ϵ_{max} and ϵ_{min} too far apart virtually any point of the series is recurrent, yielding a completely full SRP which conveys no information. On the other hand, if ϵ_{max} is too small (or, also, if ϵ_{max} and ϵ_{min}

are too close) there would be so few black pixels in the corresponding SRP that statistical quantifiers would not be worth considering. We estimate optimal values for the cutoff radius using a procedure we will describe in Sec. V.

Taking these cautionary remarks into account, it turns out that a large number of isolated and scattered points in the SRP is a strong indicator of spatial disorder. Conversely, the presence of regular structures is a fingerprint of spatially correlated clusters of points and thus of smoother spatial patterns. From the point of view of interpretation of mammographic images, however, our focus is rather on the pattern changes induced by benign or malign lesions.

These pattern changes can be identified through recurrence quantification analysis methods originally developed for time recurrence plots.[9] One of the quantifiers is the spatial recurrence rate, which is the fraction of recurrent points in a given SRP. Starting from a given element of the original matrix x_{ij} we compute the spatial recurrence sub-matrix between the element and its N neighbors (along a line or a column) obtaining $(R_{mn})_{ij}$, with $m, n = 1, \ldots N$. Hence there is one different matrix for each element of the original recurrence matrix. We obtain a spatial recurrence rate matrix as

$$\rho_{s[i,j]} = \frac{1}{N^2} \sum_{m,n=1}^{N} (R_{mn})_{ij}, \tag{3}$$

for a sub-matrix of variable size $N \times N$ and a suitably chosen cutoff radii [Fig. 1].

The extreme sensitivity to spatial differences displayed by the spatial recurrence rate matrix makes it a valuable diagnostic tool for visualization of subtle pattern changes, like borderlines virtually invisible to the naked eye, as illustrated by Fig. 2. Multiple gray disks superimposed on a gray background are practically invisible because the pixels of the disks differ from the background by a small quantity [Fig. 2(a)]. The corresponding spatial recurrence rate matrix, however, is capable to distinguish the contours of these disks due to the relatively small values of the recurrence rate at the contours with respect to the uniform background [Fig. 2(b)].

Another quantitative characterization of SRPs is based on a detailed analysis of the large and small-scale patterns or structures: (i) diagonal structures which reflect similar local behavior of different parts of the spatial pattern;[17,18] (ii) vertical structures (black lines) represent patterns which do not change along the lattice, e.g., as it typically happens in intermittency.[19,20] For notational simplicity we will call simply by R_{ij} the elements of the spatial recurrence matrix.

Diagonal lines are structures parallel to the line of identity $R_{i,i} = 1$ and formally defined as

$$R_{i+k,j+k} = 1, \quad (k = 1, 2, \ldots, \ell), \quad R_{i,j} = R_{i+\ell+1,j+\ell+1} = 0, \tag{4}$$

where ℓ is the length of the diagonal line, occurring when a segment of a given trajectory (in phase space) runs parallel to another segment. Wherever a SRP presents a diagonal line, two pieces of a trajectory have, for a given length ℓ, similar shapes. We compute $P(\ell) = \{\ell_i; i = 1, 2, \ldots N_\ell\}$, which is the frequency distribution of the lengths ℓ_i of diagonal lines, and N_ℓ is the absolute number of diagonal lines, with the exception of the main diagonal line which always exist by construction.

In analogy with time recurrence plots, we can compute the spatial determinism (a term coined in RPs involving time series), which is the fraction of points in a SRP belonging to diagonal lines, given by

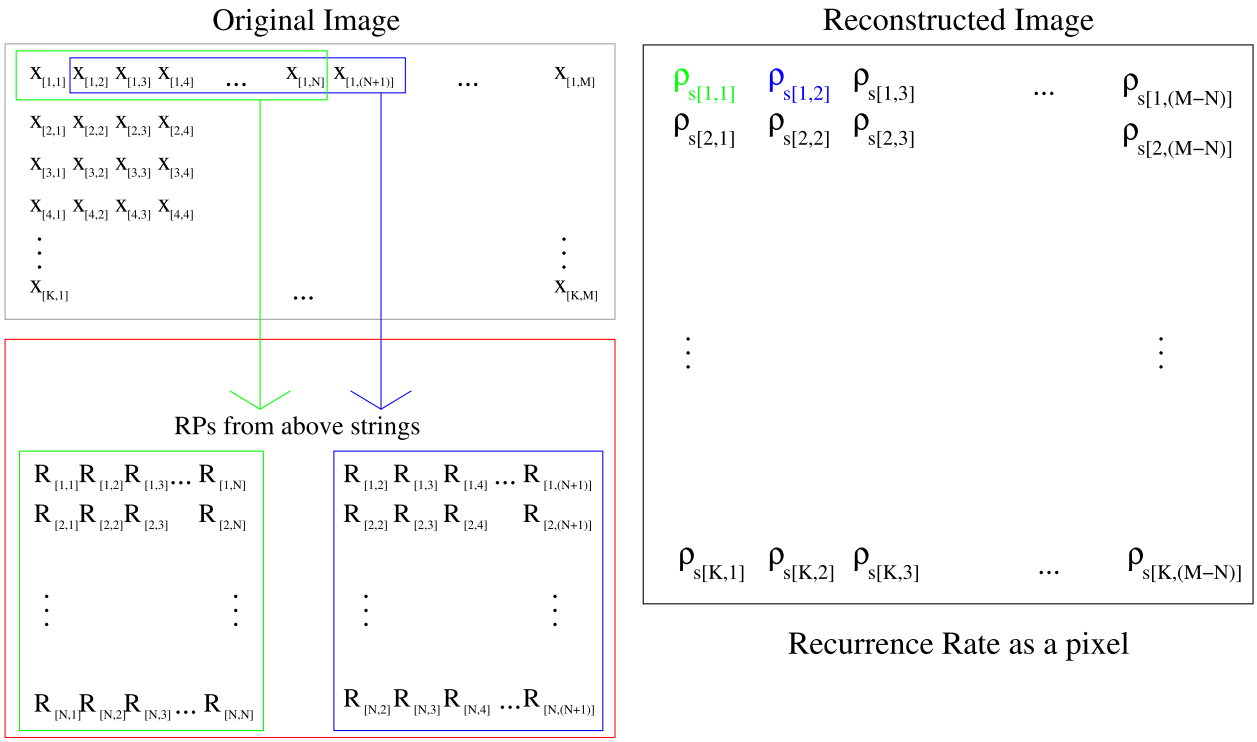

FIG. 1. Schematic figure showing the numerical method used to compute the recurrence-based diagnostic matrices from the image matrix corresponding to the digitally scanned mammography.

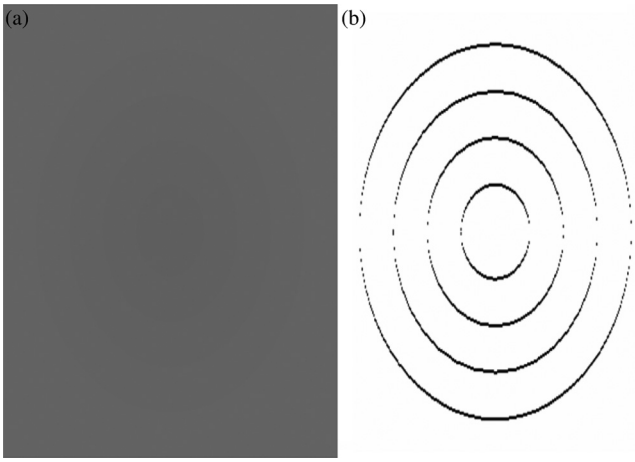

FIG. 2. (a) Gray disk against a gray background; (b) corresponding spatial recurrence rate matrix.

$$\delta_{s[i,j]} = \frac{\sum_{\ell=\ell_{min}}^{\ell_{max}} \ell P(\ell)}{\sum_{\ell=1}^{\ell_{max}} \ell P(\ell)}, \tag{5}$$

where ℓ_{min} is the minimum length allowed for a diagonal line. Its value depends on N, and in our case a good choice is $\ell_{min} = 8$. Moreover the maximum diagonal length is $\ell_{max} = N - 1$. As with the recurrence rate, we use variable size sub-matrices (lines or columns) starting at each point (i,j) of the original figure and obtain a spatial determinism matrix $\delta_{s[i,j]}$ with the same dimensions as the recurrence rate matrix.

Horizontal structures are equally useful in symmetric recurrence plots, such that it suffices to consider those vertical structures found in SRPs. Vertical structures are sequences of black pixels $R_{[i,j]}(\ell)$ such that, for a k-th vertical structure, the inequality

$$R_{i,k}(\ell)R_{i,k+1}(\ell) + R_{i,k}(\ell)R_{i,k-1}(\ell) > 0, \tag{6}$$

holds for the corresponding value of i.[19] The number of black pixels in the k-th vertical structure will be denoted as v_k. Vertical structures represent highly correlated strings of points in the SRP, and thus their appearance signals the existence of spatially coherent regions in the actual spatial pattern. Since there are typically many vertical structures in a SRP we compute the corresponding frequency distribution $P(v_k)$.

The spatial laminarity is the fraction of pixels belonging to vertical structures in a SRP

$$\lambda_{s[i,j]} = \frac{\sum_{v_k=v_{min}}^{v_{max}} v_k P(v_k)}{\sum_{v_k=1}^{v_{max}} v_k P(v_k)}, \tag{7}$$

where the minimum length of a vertical structure, v_{min}, has been chosen to be equal to 8, as for diagonal structures. Moreover the maximum vertical length is $v_{max} = N–1$. Just like we proceed with diagonal lines, we use variable-size sub-matrices and construct a spatial laminarity matrix $\lambda_{s[i,j]}$.

The procedures described above can be used to characterize pattern changes in mammographic images, but we can further refine this analysis so as to obtain even better image characterization, as it will be explained in Sec. III.

III. BLOCK RECURRENCE ANALYSIS

Instead of using line (or column) recurrences, as explained in Sec. II, we can also extract blocks of $N \times N$ elements from the spatial recurrence matrix (N is assumed to be an odd integer). The spatial series is then obtained from the elements of these blocks, and the corresponding spatial recurrence matrix can be computed by comparing the values of the block elements with the central element of the block. An example of the procedure is depicted schematically in Fig. 3. Formally the elements of the spatial recurrence rate matrix are given by

$$\rho_{b[m,n]} = \frac{1}{N^2} \sum_{i=m}^{m+N-1} \sum_{j=n}^{n+N-1} \Theta\left(|x_{[i,j]} - x_{[m+(N-1)/2,n+(N-1)/2]}| - \epsilon_{min}\right) \times \Theta\left(\epsilon_{max} - |x_{[i,j]} - x_{[m+(N-1)/2,n+(N-1)/2]}|\right). \tag{8}$$

In the analysis of block recurrence matrices we make a local average of the elements in the original image, hence for the spatial recurrence matrix obtained using Eq. (8) there is no longer a well-defined interpretation for the determinism or laminarity, as in the case where line (or column) recurrences were considered. The advantage of taking block recurrence rate elements instead of line (or column)

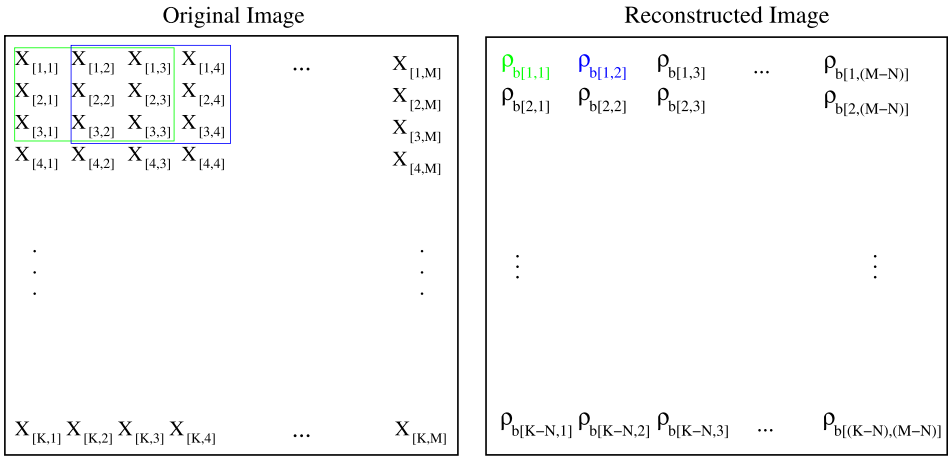

FIG. 3. Schematic figure showing the numerical method used to compute the recurrence-based diagnostic matrices from the image matrix corresponding to the digitally scanned mammography. The first image shows the original image and how we extracted blocks of elements for computing the spatial recurrence matrix, from which the elements of the recurrence rate matrix are obtained (reconstructed image).

recurrences is illustrated in Fig. 4, where the same reconstruction is performed in the image previously reconstructed by lines [Fig. 2]. Comparing both cases we observe a better definition of the disk contours by using the block recurrence rate matrix, whereas the line-recurrence has some loss of definition in the contours due to the way we scanned the lines of the recurrence matrix.

IV. BLOCK-RECURRENCE ANALYSIS OF MAMMOGRAPHIC IMAGES

Now we are in position of using the block-recurrence quantifier, namely, the recurrence-rate matrix given by Eq. (8), to interpret mammographic images. The latter were obtained from the database made available by the LAPIMO (Laboratory of Analysis and Processing of Medical and Odontologic Images) of the São Carlos School of Engineering, University of São Paulo, Brazil.[11]

The breast images were obtained with a LUMISYS scanner with 150 μ-resolution. The original files are stored in *tiff* format of integer quantization values. In the image processing field, it is used the quantization term to define the values attributed for each pixel,[12,13] and it holds the light intensity fixed for a specific channel of color. Commonly in mammography it is used just one channel with up to 16 bits of quantization (what gives 2^{16} levels of quantization) in grayscale, what is very good due to the evident contrast differences. However it is also possible to obtain a RGB processed image using 3 channels with 8 bits of quantization levels per channel. This gives 256 levels of red, green, and blue, such that in the sum the RGB have 2^{24} quantization levels.

An original high-resolution image taken from the LAPIMO database, in grayscale and scanned with 12 bits resolution (yielding 4096 quantization levels), is shown in Fig. 5(a). In Fig. 5(b) we show the reconstructed image using a conventional method (Sobel filtering), showing a barely visible edge corresponding to the actual breast contour. The use of a block-recurrence rate matrix [using $\epsilon_{min} = 0.0012$, $\epsilon_{max} = 0.03$ and square blocks with size $N = 25$] yields a much better reconstructed image, not only for the breast contour but also the variations of density near the contour as well as a

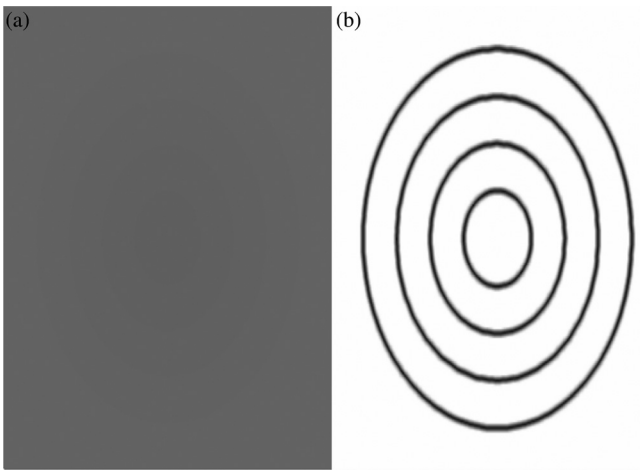

FIG. 4. (a) Gray disk against a gray background; (b) corresponding spatial recurrence rate matrix with a block-recurrence quantifier.

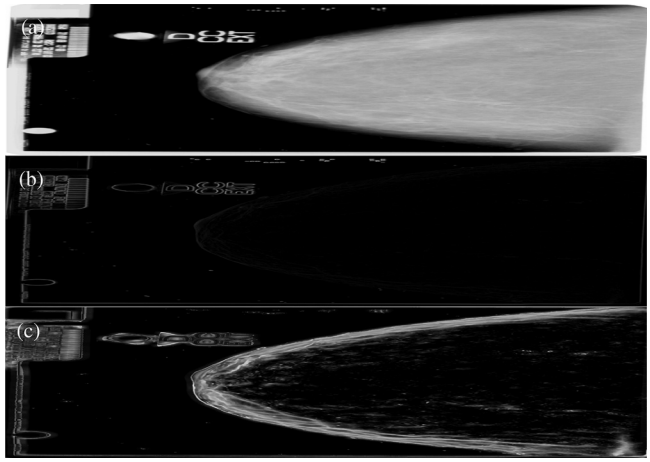

FIG. 5. (a) A high-resolution mammographic grayscale image from LAPIMO database; (b) a reconstructed image filtered with the Sobel filter; (c) a reconstructed image obtained from the block recurrence rate matrix with $\epsilon_{min} = 0.0012$, $\epsilon_{max} = 0.03$, and square blocks with size $N = 25$.

number of internal structures, some of them very small and barely distinguishable by naked eye from the original image [Fig. 5(c)].

The ability displayed by the block-recurrence matrix to detect subtle pattern changes in mammographies encourages one to apply it to detect internal structures, an example being depicted in Fig. 6. The original image, with resolution of 10^{12} quantizations [Fig. 6(a)], is reconstructed using recurrence rate matrix with 25×25 blocks and where we keep $\epsilon_{max} = 0.0030$ at a fixed value and vary ϵ_{min} from 0.0012 [Fig. 6(b)] to 0.0028 (bottom) [Fig. 6(f)]. As a general trend in these pictures, the smaller the value of ϵ_{min} the better we resolve small structures in the original image. Actually the resolution is improved as the difference $\epsilon_{max} - \epsilon_{min}$ increases. In Sec. V we shall discuss a systematic method to obtain "optimal" values of the cutoff radii.

In particular, many of these structures may be micro-calcifications whose identification would depend also from the expertise of a trained specialist. As an example, in Fig. 7(a) we show a zoomed image of a region of the reconstructed image in Fig. 6(b) (the best resolution we have gotten), chosen because there is a set of suggestive structures that may be micro-calcifications, that are practically invisible to the naked eye in the original mammographic image [cf., Fig. 6(a)]. In Fig. 7(b) another zoomed region of the reconstructed image is shown, with a suggestive presence of channeled calcifications.

That the decrease in the cutoff radius difference actually improves the observation of internal micro-structures in mammographic images is confirmed by the analysis shown in Fig. 8, where the original image is in the top of the figure, and the figures below refer to reconstructed images (using block-recurrence-rate matrices) using different values of ϵ_{min}, keeping $\epsilon_{max} = 0.0030$.

V. ANALYSIS OF CUTOFF RADII

A key question in applying the current methods to mammographic digital image analysis is how to choose in an adequate way the cutoff radii ϵ_{max} and ϵ_{min}. If their values are

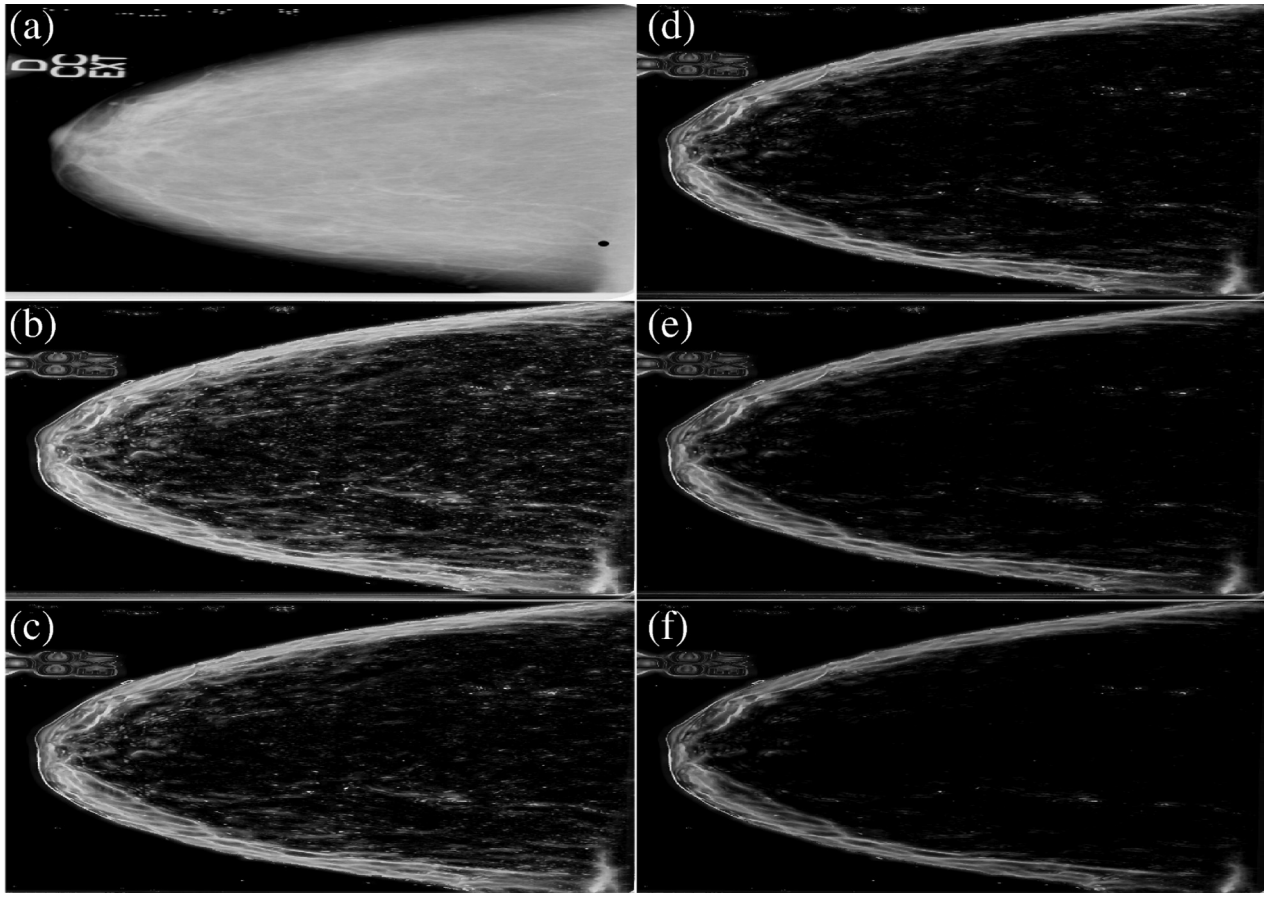

FIG. 6. (a) A high-resolution mammographic grayscale image from LAPIMO database; reconstructed images obtained with block recurrence-rate matrices with $N = 25$, $\epsilon_{max} = 0.0030$, and $\epsilon_{min} = 0.0012$ (b), 0.0016 (c), 0.0020 (d), 0.0024 (e), and 0.0028 (f).

chosen too close to each other, we may have too few recurrences to justify a statistical analysis, and if they are chosen too far apart (or if ϵ_{max} is too large) we may have a large number of false recurrences. In both cases the reliability of the method would be jeopardized by a strong dependence on some arbitrary parameter.

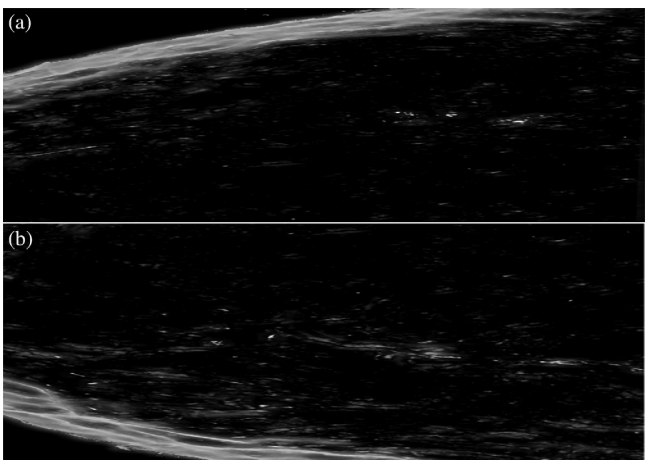

FIG. 7. (a) and (b) Zoomed regions of the original mammographic image depicted in Fig. 6, showing internal structures suggestive of microcalcifications.

We developed a systematic procedure for choosing the optimal value of the cutoff radius. We choose two initial values for ϵ_{min} and ϵ_{max}, namely, 2×10^{-6} and 4×10^{-6}, and construct the recurrence matrix in such a way that two points of a spatial series are considered as recurrent only if $\epsilon_{min} < |x(i) - x(j)| < \epsilon_{max}$. The spatial recurrent matrix R_{ij} is constructed from these values of ϵ, and we compute the average spatial recurrence rate for that value of ϵ. Since we are treating here block-recurrence matrices, a convenient quantity to compute is

$$OPT_{\delta}(\epsilon_{mean}) = \frac{\sum_{s=1}^{K-N} \sum_{t=1}^{M-N} \rho_{b[s,t]}}{(K-N+1)(M-N+1)}. \tag{9}$$

The next step is to increase both ϵ_{min} and ϵ_{max} by tiny amounts: $\delta_{min} = 2 \times 10^{-6}$ for ϵ_{min} and $\delta_{max} = 4 \times 10^{-6}$ for ϵ_{max}. We then repeat the calculation of the above quantity, and so on. In this way we can plot the variable OPT_{δ}, for instance, as a function of $\epsilon_{mean} = (\epsilon_{max} + \epsilon_{min})/2$, as shown in Fig. 9. We then choose the optimal value of ϵ_{mean} as the local minimum of these curves (in the case of Fig. 9 the local minimum of all curves seems to be *circa* 4×10^{-4}). Once we assign a given optimal value for ϵ_{opt} we choose the refined values of ϵ_{max} and ϵ_{min} such that $\epsilon_{min} < \epsilon_{mean} < \epsilon_{max}$.

Figures 9(a) and 9(b) refer to the images depicted in Figs. 6(a) and 8(a), respectively. It is a noteworthy feature

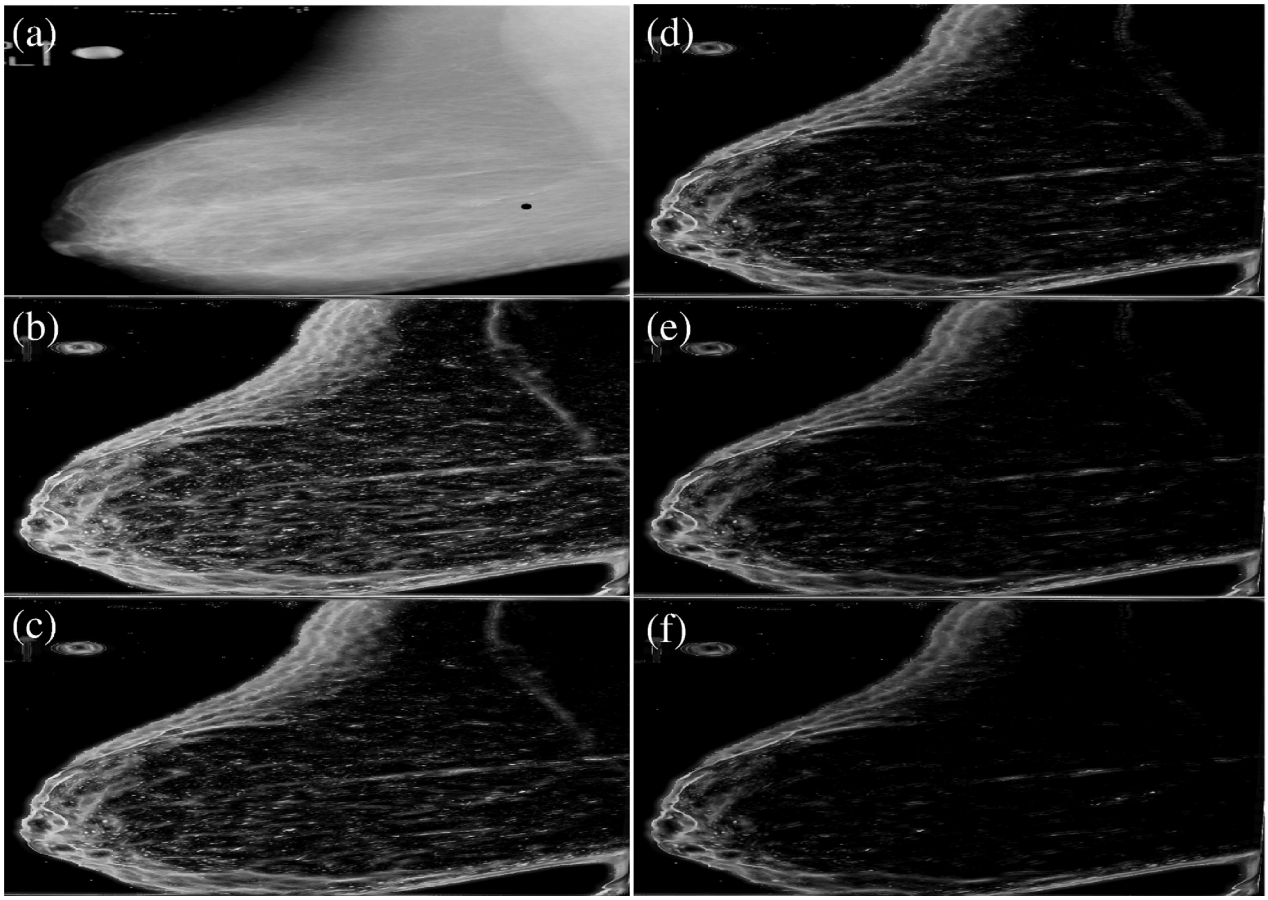

FIG. 8. (a) A high-resolution mammographic grayscale image from LAPIMO database; reconstructed images obtained with block recurrence-rate matrices with $N = 25$, $\epsilon_{max} = 0.0030$, and $\epsilon_{min} = 0.0012$ (b), 0.0016 (c), 0.0020 (d), 0.0024 (e), and 0.0028 (f).

that for both images the variation of OPT_δ was very similar, such that we have chosen the same minimum for the ϵ_{opt} to be used in the reconstructed images.

Finally we remark that the similarity between the curves of OPT_δ obtained from different images is in fact a characteristic feature of the scanner used to obtain the images. As a consequence, the procedure we described here can be used only once, as we obtain multiple images from the same scanner, which saves processing time, and allowing faster results.

VI. CONCLUSIONS

In conclusion, we propose the use of spatial recurrence plots as a means for detecting structures in digital mammographies which would be otherwise hardly visible. Spatial

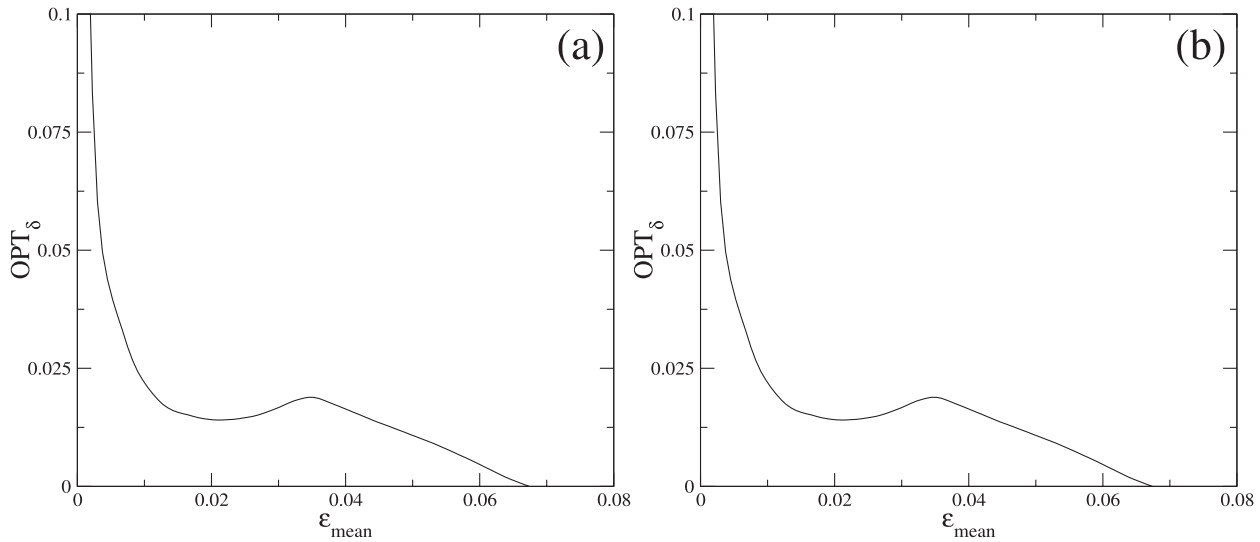

FIG. 9. Average values of the recurrence rates as a function of the cutoff radius for Figs. 6(a) and 8.

recurrence plots were inspired in the temporal recurrence properties of time series that have been studied since the work of Poincaré at the end of 19th century. In fact the exploitation of time recurrences has led to a number of important results in the characterization of the dynamics of system generating the time series. A straightforward application of this analogy to spatial profiles (at fixed time) corresponds to make a line of column scanning of some raw image, and the results show promising results, unless the boundaries of the structures to be analyzed are nearly tangent to vertical and/or horizontal lines of the reconstructed image.

A possible way to circumvent this problem has been to use block-recurrence based spatial plots, with which it has been proved possible to detect very subtle structures in digitized images that are utterly invisible to a naked eye. This property has encouraged us to apply these techniques to the analysis of medical images, like mammographies, where the early detection of cancer is facilitated by the identification of small structures like micro-calcifications within the lipidic tissue of the breast. Since identification of these structures often leads to a sometimes alarming number of both false negatives and false positives, it is our opinion that the recurrence technique we propose is a useful tool in the toolbox of the physician responsible to the diagnostic of mammographic images.

Our method has been shown to be as reliable as conventional image treatment techniques, but with a considerably smaller computer time. This issue is particularly important so as to give faster results to the women undergoing mammographies (conventional digital image treatment takes a large computer time to give good quality results). The spatial recurrence techniques so proposed are not restricted, however, to mammography analysis but can be applied in other pattern recognition and characterization tasks, as in micrography analysis, topographical exploration and other applications which require fast computer processing and reliability.

ACKNOWLEDGMENTS

This work was made possible with partial financial help from CNPq, CAPES, and Fundação Araucária (Brazilian Government Agencies).

[1]See http://www.mammoimage.org/general-info/ for general information on the analysis of digital images from mammographies, articles, methods and recent advances in this area.
[2]Y. Jiang, R. M. Nishikawa, R. A. Schmidt, C. E. Metz, M. L. Giger, and K. Doi, Acad. Radiol. **6**, 22 (1999).
[3]K. Doi, H. MacMahon, S. Katsuragawa, R. M. Nishikawa, and Y. Jiang, Eur. J. Radiol. **31**, 97 (1999).
[4]R. M. Nishikawa, M. L. Giger, K. Doi, C. J. Vyborny, and R. A. Schmidt, Med. Phys. **20**, 1661 (1993).
[5]F. F. Yin, M. L. Giger, K. Doi, C. E. Metz, C. J. Vyborny, and R. A. Schmidt, Med. Phys. **18**, 955 (1991).
[6]W. Zhang, K. Doi, M. L. Giger, R. M. Nishikawa, and R. A. Schmidt, Med. Phys. **23**, 595 (1996).
[7]D. B. Vasconcelos, S. R. Lopes, R. L. Viana, and J. Kurths, Phys. Rev. E **73**, 056207 (2006).
[8]N. Marwan, J. Kurths, and P. Saparin, Phys. Lett. A **360**, 545 (2007).
[9]N. Marwan, M. C. Romano, M. Thiel, and J. Kurths, Phys. Rep. **438**, 237 (2007).
[10]F. A. S. Silva, R. L. Viana, T. L. Prado, and S. R. Lopes, Comm. Nonlin. Sci. Numer. Simulat. **19**, 1055 (2014).
[11]See http://lapimo.sel.eesc.usp.br/bancoweb/ for details on the obtention of the raw images used in this work.
[12]B. Jhne, *Digital Image Processing*, 5th ed. (Springer-Verlag, Heidelberg, 2002).
[13]R. F. Gonzales, R. E. Woods, and S. L. Eddins, *Digital Image Processing Using MATLAB*, 2nd ed. (Gatesmark Publishing, 2009).
[14]*Biomedical Image Processing*, edited by T. M. Deserno (Springer-Verlag, Berlin, 2011).
[15]M. Heath, K. Bowyer, D. Kopans, R. Moore, and W. P. Kegelmeyer, "The digital database for screening mammography," in *Proceedings of the Fifth International Workshop on Digital Mammography*, edited by M. J. Yaffe (Medical Physics Publishing, 2001), pp. 212–218.
[16]M. Heath, K. Bowyer, D. Kopans, W. P. Kegelmeyer, R. Moore, K. Chang, and S. MunishKumaran, "Current status of the digital database for screening mammography," in *Proceedings of the Fourth International Workshop on Digital Mammography* (Kluwer Academic Publishers, 1998), pp. 457–460.
[17]J. P. Zbilut and C. L. Webber, Jr., Phys. Lett. A **171**, 199 (1992).
[18]L. L. Trulla, A. Giuliani, J. P. Zbilut, and C. L. Webber, Jr., Phys. Lett. A **223**, 255 (1996).
[19]N. Marwan, N. Wessel, U. Meyerfeldt, A. Schirdewan, and J. Kurths, Phys. Rev. E **66**, 026702 (2002).
[20]N. Marwan and J. Kurths, Phys. Lett. A **302**, 299 (2002).